Scientific Papers. Series E. Land Reclamation, Earth Observation & Surveying, Environmental Engineering. Vol. XV, 2026
Print ISSN 2285-6064, CD-ROM ISSN 2285-6072, Online ISSN 2393-5138, ISSN-L 2285-6064

COMPARATIVE ASSESSMENT OF ANNUAL DYNAMICS IN WATER QUALITY OF HERASTRAU LAKE, ROMANIA

Iuliana VOICU[1], Mihaela DRAGOI CUDALBEANU[1], Andreea Adriana MAN[1], Nicoleta Daniela SARBU[1], Teodor COSTACHIOIU[2], Daniela FAUR[2], Carmen Laura CIMPEANU[1]

[1]Faculty of Land Reclamation and Environmental Engineering, University of Agronomic Sciences and Veterinary Medicine of Bucharest, 59 Marasti Blvd, 011464, District 1, Bucharest, Romania
[2]National University of Science and Technology Politehnica, 060042, Bucharest, Romania

Corresponding author emails: mihaela.dragoi@fifim.ro, daniela.faur@upb.ro

Abstract

Water quality assessment is vital to environmental management. Regular monitoring of lakes helps protect environmental integrity and human health. This study assessed annual changes in water quality in Herastrau Lake (Bucharest, Romania) using field and laboratory measurements complemented by satellite observations. Water samples were collected from ten sites in autumn 2024 and spring 2025 and analyzed for pH, electrical conductivity, total dissolved solids, salinity, dissolved oxygen, turbidity, chloride, nitrite, nitrate, ammonium, total suspended solids, hardness, and iron. Results were compared with Romanian standards (Order No. 161/2006), and Pearson correlations were performed. The lake remained alkaline in both years (pH 8.50), while dissolved oxygen declined markedly in 2025 (2.59 mg/L) compared with 2024 (6.82 mg/L). Turbidity exceeded 5 NTU, and ammonium nitrogen showed elevated concentrations (12.07 mg N-NH_4^+/L in 2024; 13.50 mg N-NH_4^+/L in 2025), suggesting persistent eutrophication pressure. Sentinel-2 imagery (10–20 m) was used to estimate surface turbidity from red-edge reflectance, with NDWI used for water masking*, and the results were validated with laboratory data. The water quality underscores the need for targeted pollution control measures.*

Key words*: eutrophication, Herastrau, Romania, Sentinel-2, water quality.*

INTRODUCTION

Although water is fundamental to life, freshwater accounts for only 2.5% of the global water volume, and just 1% is accessible for use, with much of it sequestered in reservoirs. In this context, lakes are a vital yet strictly finite resource (Hoggang & Reyes, 2023). Beyond serving as critical water reservoirs, lakes support diverse ecosystems and play a vital role in regulating local microclimates (K. Zhang et al., 2025) and stabilizing the climate by driving atmospheric carbon fixation through phyto-plankton photosynthesis (Oustani et al., 2026).

Freshwater lakes are highly sensitive to both natural factors and anthropogenic pressures (urbanization, industrialization, agriculture) that compromise their ecological integrity (Liu et al., 2025). Nutrient enrichment fundamentally alters water quality, trophic status, and biological community structure. Because plankton communities respond quickly to these fluctuations, they serve as reliable indicators of changing ecological conditions (Nkhata et al., 2026). Ultimately, excessive chemical inputs alter water physicochemical parameters, triggering eutrophication, characterized by elevated phytoplankton biomass, harmful cyanobacterial blooms, reduced transparency, and oxygen depletion (Nkhata et al., 2026; Oustani et al., 2026).

Eutrophication is the enrichment of water with nutrients like nitrogen and phosphorus, leading to excessive algae and plant growth. As organic matter decomposes, oxygen levels drop, causing fish kills, biodiversity loss, reduced water clarity, and harmful cyanobacterial blooms that release toxins. It damages water ecosystems and recreation and is a major global threat to inland water quality (Zhou et al., 2024; Morelato et al., 2026).

Urban lakes provide vital ecosystem services and serve as structural components of the metropolitan landscape. They enhance urban environmental quality by providing reliable access to clean water for both functional use and

recreation (Cheval et al., 2020). An example of a metropolitan ecosystem facing localized pressures is Herastrau Lake, located in the northern district of Bucharest, Romania. It is an artificial water body and a key component of the anthropogenic lake cascade along the Colentina River. Herastrau Lake is particularly exposed to eutrophication, as it receives continuous anthropogenic nutrient loads from urban runoff, sewage inputs, and atmospheric deposition, while also providing important recreational, aesthetic, microclimatic, and biodiversity services to a densely populated city. However, its location within a densely populated area subjects it to ongoing environmental challenges, including urban surface runoff and localized waste generation.

Despite its ecological and recreational importance, comprehensive data regarding the status of this aquatic system remain insufficient, with only a limited number of local studies examining water pollution in Herastrau Lake. To address this critical knowledge gap, this study aims to assess the lake's physico-chemical profile and quantify its current state of degradation. Specifically, this research monitors key environmental indicators - including pH, electrical conductivity, turbidity, and chloride ions - alongside critical nutrient loadings - namely, ammonia, nitrites, nitrates, and phosphates - to assess the immediate urban impact footprint.

MATERIALS AND METHODS

Water Site and Sampling Points Description

Water sampling was conducted at ten sites distributed across Herastrau Lake during two monitoring campaigns, on 21 October 2024 (autumn) and 11 March 2025 (early spring). The same sampling locations were used in both campaigns, and their geographic coordinates were recorded to ensure spatial consistency and enable direct comparison between the two monitoring periods. At each site, selected physicochemical parameters were measured in situ, and additional analyses were performed in the laboratory afterward. This combined approach allowed assessment of both spatial variability in water quality across the lake and seasonal differences between the autumn 2024 and early spring 2025 campaigns.

Water Sampling and Physicochemical Analyses

Water sampling was conducted in accordance with the Romanian guidelines for water sampling from natural and artificial lakes (ISO 5667-4:2016). Water was manually collected at approximately 0.5 m below the surface and placed in polyethylene containers, then immediately stored in a refrigerated transport box at approximately 4°C until arrival at the laboratory. Before laboratory analyses, samples were allowed to reach room temperature, as required by the analytical procedure.

Water temperature, pH, electrical conductivity (EC), total dissolved solids (TDS), salinity, and dissolved oxygen (DO) were measured in situ at each sampling location using a calibrated portable multiparameter. The remaining physicochemical parameters were determined in the laboratory within 24-48 h of sample collection.

Turbidity was measured with a calibrated turbidimeter and reported in nephelometric turbidity units (NTU). Total suspended solids (TSS) were measured gravimetrically by filtering homogenized water through pre-dried, pre-weighed filter paper. The filter was dried at 105 °C, cooled, and reweighed. TSS was calculated from the mass difference and given as mg/L.

Chloride (Cl^-) concentrations were determined by Mohr titration with a standardized silver nitrate ($AgNO_3$) solution, using potassium chromate (K_2CrO_4) as the endpoint indicator. Total hardness (TH) was determined by complexometric titration with disodium ethylenediaminetetraacetate (EDTA), using Eriochrome Black T as the endpoint indicator. Temporary hardness (CH) was determined by titration with hydrochloric acid (HCl) using methyl orange as the endpoint indicator, while permanent hardness (NCH) was calculated as the difference between TH and CH.

Nitrite ($N\text{-}NO_2^-$) and ammonium ($N\text{-}NH_4^+$) were determined spectrophotometrically at 540 and 650 nm, respectively, according to the procedures described by Sandu et al. (2023). Nitrate ($N\text{-}NO_3^-$) was not measured directly; instead, nitrate-equivalent concentrations were calculated from nitrite values using the corresponding stoichiometric conversion factor. Nitrogen species results were expressed as mg

N/L. Iron (Fe^{3+}) was determined spectrophotometrically using the potassium thiocyanate (KSCN) method at 490 nm. Fe^{3+} concentrations were expressed as mg Fe^{3+}/L.
All analytical instruments were calibrated before measurements, following the respective procedures, to maintain data quality and accuracy. Laboratory determinations were performed in triplicate, and the results were expressed as mean ± standard deviation (SD).

Water Quality Classification
The physicochemical quality of Herastrau Lake water was evaluated by comparing measured parameters with threshold values established by the Romanian regulatory framework for surface-water monitoring (Order No. 161/2006). According to this classification system, surface waters are divided into five quality classes (I-V), ranging from high-quality waters (Class I) to heavily degraded waters (Class V). For each sampling point and monitoring year, the measured concentrations of dissolved oxygen (DO), chlorides (Cl^-), nitrite ($N\text{-}NO_2^-$), nitrate ($N\text{-}NO_3^-$), ammonium ($N\text{-}NH_4^+$), and iron (Fe^{3+}) were compared with the corresponding class-specific threshold values. This approach allowed evaluation of both spatial variability among the ten sampling sites and interannual changes between 2024 and 2025. The resulting classification was used to identify the physico-chemical parameters primarily responsible for deteriorating lake-water quality and to assess changes in water-quality conditions between the two monitoring campaigns.

Statistical Analysis and Pearson Correlation
Statistical analysis of the water-quality data was performed using GraphPad Prism (version 11.0.2). Pearson's correlation coefficient was used to evaluate the relationships among water temperature, pH, electrical conductivity (EC), total dissolved solids (TDS), salinity, dissolved oxygen (DO), turbidity, chlorides (Cl^-), total hardness (TH), temporary hardness (CH), permanent hardness (NCH), nitrite ($N\text{-}NO_2^-$), nitrate ($N\text{-}NO_3^-$), ammonium ($N\text{-}NH_4^+$), total suspended solids (TSS), and iron (Fe^{3+}).

Satellite data set description
Satellite data consisted of Sentinel-2 MSI Level-2A products with atmospherically corrected bottom-of-atmosphere surface reflectance (tile T35TMK). For each campaign, the two cloud-free scenes closest to the sampling date were selected - 21 and 26 October 2024 for the autumn campaign, and 5 and 20 March 2025 for the early-spring campaign - yielding four scenes in total. Prior to analysis, cloud-, shadow-, and cirrus-affected pixels were removed using the Scene Classification Layer (SCL). Because the strict SCL water class (class 6) frequently misclassifies the turbid, chlorophyll-rich water of eutrophic lakes as vegetation or bare soil, and because the sampling locations were independently verified to lie over open water, SCL classes 4-7 (vegetation, bare soil, water, and unclassified) were retained at the sampling points. The radiometric offset introduced in processing baseline 04.00 was then applied to recover surface reflectance. For every sampling point, a per-point median composite was computed from the two scenes of the corresponding campaign. The median was preferred over single-date extraction to reduce residual cloud/haze contamination and transient surface effects, while keeping the reflectance temporally close to the in-situ measurements. Spectral indices and band ratios were subsequently derived and extracted at the ten-point locations for comparison with the in-situ data.

Satellite-based assessment of water turbidity
Turbidity is an optically active water-quality parameter: suspended particles raise the water-leaving reflectance in the red and near-infrared (NIR) regions, where clear water is otherwise strongly absorbing, and the magnitude of this increase scales with the concentration of suspended matter. The red-to-NIR portion of the Sentinel-2 spectrum is therefore the most informative for turbidity retrieval.
The following bands were evaluated as turbidity predictors, as shown in Table 1: the red band B04 (665 nm) and the first red-edge band B05 (705 nm), which respond at low-to-moderate turbidity; and the red-edge band B07 (783 nm) together with the NIR band B08 (842 nm), which remain sensitive at high turbidity, where the red band tends to saturate, a behavior analogous to the band-switching logic of semi-analytical turbidity models. In addition to the individual bands, two red-edge-to-red ratios

were computed, re5_red = B05/B04 and re7_red = B07/B04, since band ratios largely cancel multiplicative effects (illumination geometry, residual atmospheric scattering, and the imperfect Level-2A correction over water) and thus provide more robust proxies than single bands. All candidate predictors listed in Table 1 were screened against the in-situ measurements, and the band that showed the strongest and most consistent association with turbidity in both campaigns, the red-edge band B07, was retained for calibration; NDTI is additionally reported below because it is the only index among the candidates explicitly formulated for turbidity.

Table 1. Sentinel-2 bands and spectral indices evaluated for turbidity retrieval

Band/ Spectral index	Definition	Role for turbidity
B04 (red)	665 nm	Suspended sediment; low-to-moderate turbidity
B05 (red-edge 1)	705 nm	Red-edge response across the turbidity range
B07 (red-edge 3)	783 nm	Sensitive at high turbidity (red saturates)
B08 (NIR)	842 nm	High-turbidity/ TSS signal
re5_red	B05/B04	Red-edge/red ratio; robust at low-to-moderate values
re7_red	B07/B04	Red-edge/red ratio; **candidate predictor**
NDTI (Lacaux et al., 2007)	(B04−B03)/ (B04+B03)	Normalized Difference Turbidity Index
NDWI (McFeeters, 1996)	(B03−B08)/ (B03+B08)	Water masking only

Calibration of the satellite-derived turbidity

Calibration of the satellite turbidity proxy was carried out as a spatial regression across the ten sampling points, relating the in-situ turbidity of each campaign to the corresponding median Sentinel-2 reflectance values and band ratios extracted at the same locations. Because the analysis compares spatially distributed point pairs rather than a dense temporal series and given the small sample size (n = 10), the strength and significance of each candidate predictor were assessed using both the Pearson correlation coefficient (r), which quantifies the strength of a linear association, and the Spearman rank correlation coefficient (ρ), which captures monotonic relationships and is more robust to non-linearity, non-normality and outliers.

Reporting both coefficients allows assessment of each relationship's linearity: close agreement between r and ρ indicates a robust, approximately linear association, whereas marked divergence signals non-linearity or sensitivity to individual points. For n = 10, the critical value for significance at $p < 0.05$ (two-tailed) is $|r| \approx 0.63$; all results were therefore treated as exploratory.

RESULTS AND DISCUSSIONS

Spatial Distribution of Sampling Points

The ten georeferenced sampling points spanned different areas of Herastrau Lake, ensuring adequate spatial representation of the water body. Table 2 lists the geographical coordinates of the sampling sites, and Figure 1 shows their spatial distribution across Herastrau Lake. The same locations were monitored in 2024 and 2025, enabling a consistent assessment of spatial and temporal variations in water quality.

Table 2. Geographical coordinates of the sampling points in Herastrau Lake

Point	Latitude (N)	Longitude (E)
P1	44°28'39.54252"	26°4'34.83156"
P2	44°28'52.00000"	26°4'30.00000"
P3	44°28'56.60544"	26°4'41.02500"
P4	44°29'13.04952"	26°4'57.93348"
P5	44°28'56.56080"	26°4'56.75412"
P6	44°28'40.74636"	26°4'42.59460"
P7	44°28'39.43344"	26°5'10.15080"
P8	44°28'31.52316"	26°5'19.74228"
P9	44°28'22.28196"	26°4'53.78880"
P10	44°28'28.08360"	26°4'39.84672"

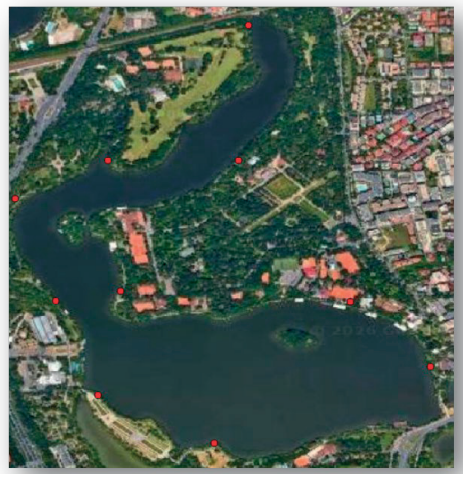


Figure 1. Spatial distribution of the water sampling sites in Herastrau Lake, Bucharest, Romania (background: Google Earth true-color satellite imagery)

Physicochemical parameters and water-quality classification

During the autumn 2024 campaign, Herastrau Lake water was slightly alkaline, with pH values ranging from 8.17 to 8.60, while EC ranged from 331 to 547 µS/cm. Salinity ranged from 160 to 270 mg/L and TDS from 165 to 300 mg/L, indicating moderate spatial variability in the lake's dissolved ionic content. DO was relatively favorable, ranging from 5.81 to 7.61 mg O_2/L. Based on the water-quality classification, five sampling points (P1, P4, P5, P8, and P9) were assigned to Class I, three points (P2, P3, and P7) to Class II, and only P6 and P10 to Class III. Turbidity ranged from 5.04 ± 0.98 to 14.80 ± 0.23 NTU, with the highest value at P2, suggesting localized differences in suspended particulate matter (Table 3).

Cl^- concentrations ranged from 39.45 ± 3.86 to 65.04 ± 4.73 mg/L and were consistently classified as Class I at all sampling sites. NO_2^- concentrations showed greater variability, ranging from 0.03 to 0.08 mg N-NO_2^-/L. Most sites were classified as Class II, whereas P1 and P10 reached Class III. In contrast, all NO_3^- values remained within Class I. The most pronounced deterioration was associated with NH_4^+, ranging from 9.71 ± 1.19 to 17.07 ± 1.09 mg N-NH_4^+/L and resulting in Class V at all ten sampling points. This uniform classification indicates that NH_4^+ represented the major N-related water-quality concern during the 2024 campaign. Fe^{3+} concentrations were very low (0.0002 - 0.0005 mg Fe^{3+}/L) and corresponded to Class I throughout the lake.

Table 3. Physicochemical water-quality parameters for Herastrau Lake in 2024

Point	Temperature (°C)	pH (pH units)	EC (µS/cm)	Salinity (mg/L)	TDS (mg/L)	DO (mg O_2/L)	Turbidity (NTU)	Cl^- (mg/L)
P1	16.06	8.60	388	190	194	7.10	7.47 ± 0.58	39.45 ± 3.86
P2	18.52	8.17	483	230	241	6.66	14.80 ± 0.23	54.88 ± 4.54
P3	16.11	8.22	405	200	203	6.42	10.00 ± 0.57	55.80 ± 4.91
P4	14.60	8.27	360	170	180	7.50	11.85 ± 0.49	56.29 ± 1.12
P5	16.16	8.26	331	160	165	7.05	5.04 ± 0.98	57.40 ± 4.00
P6	21.63	8.26	504	240	252	5.81	7.46 ± 0.77	41.44 ± 2.80
P7	15.73	8.34	547	270	273	6.54	8.87 ± 0.54	57.14 ± 2.99
P8	17.70	8.37	496	240	248	7.59	8.40 ± 0.66	61.12 ± 7.07
P9	16.55	8.32	520	250	260	7.61	7.34 ± 1.10	63.45 ± 6.08
P10	14.96	8.36	488	200	300	5.92	11.54 ± 0.97	65.04 ± 4.73
Point	**$N–NO_2^-$ (mg/L)**	**$N–NO_3^-$ (mg/L)**	**$N–NH_4^+$ (mg/L)**	**TSS (mg/L)**	**TH (mg/L)**	**CH (mg/L)**	**NCH (mg/L)**	**Fe^{3+} (mg/L)**
P1	0.08± 0.00	0.10 ± 0.00	9.71 ± 1.19	5.07 ± 0.20	190.66 ± 2.82	74.18 ± 0.80	116.48 ± 2.62	0.0005 ± 0.00
P2	0.04 ± 0.00	0.05 ± 0.01	13.14 ± 0.25	5.90 ± 0.26	241.13 ± 0.56	125.99 ± 0.92	115.14 ± 0.50	0.0004 ± 0.00
P3	0.04 ± 0.00	0.06 ± 0.00	11.21 ± 0.62	6.20 ± 0.18	251.23 ± 1.21	138.11 ± 0.80	113.12 ± 1.12	0.0004 ± 0.00
P4	0.05 ± 0.00	0.08 ± 0.00	17.07 ± 1.09	6.35 ± 0.71	224.31 ± 1.39	112.31 ± 0.84	112.00 ± 1.23	0.0004 ± 0.00
P5	0.03 ± 0.00	0.05 ± 0.00	11.68 ± 0.88	5.67 ± 0.31	226.55 ± 1.63	116.78 ± 0.92	109.77 ± 1.43	0.0004 ± 0.00
P6	0.04 ± 0.00	0.06 ± 0.01	10.08 ± 0.57	5.33 ± 0.58	211.97 ± 2.95	88.99 ± 0.20	122.98 ± 2.87	0.0004 ± 0.00
P7	0.03 ± 0.00	0.05 ± 0.00	11.35 ± 0.00	1.73 ± 0.08	203.00 ± 4.16	102.20 ± 0.88	100.80 ± 4.18	0.0003 ± 0.00
P8	0.03 ± 0.00	0.04 ± 0.00	12.81 ± 2.47	4.25 ± 0.30	199.64 ± 0.99	89.43 ± 0.68	110.21 ± 0.87	0.0002 ± 0.00
P9	0.06 ± 0.00	0.08 ± 0.04	11.65 ± 1.55	3.15 ± 0.13	209.73 ± 2.43	99.97 ± 0.96	109.76 ± 2.58	0.0004 ± 0.00
P10	0.08 ± 0.00	0.10 ± 0.00	12.03 ± 1.67	1.10 ± 0.02	200.87 ± 2.83	100.20 ± 0.80	100.67 ± 2.63	0.0004 ± 0.00

A distinctly different pattern was observed during the early spring 2025 campaign (Table 4). Although pH remained alkaline and comparable to 2024 (8.15-8.95), EC generally increased, reaching up to 723 µS/cm, while salinity varied between 290 and 350 mg/L. The most important change was in DO, which decreased markedly to 1.90-3.70 mg O_2/L. Consequently, all ten sampling sites were classified as Class V for DO, indicating a substantial deterioration of the lake oxygen regime compared with autumn 2024. Turbidity remained spatially heterogeneous, ranging from 4.36 ± 0.39 NTU at P1 to a maximum of 16.40 ± 0.71 NTU at P8.

Despite deteriorating oxygen conditions, Cl^- concentrations remained within Class I at all sites in 2025 (Table 5). NO_2^- concentrations were generally lower than in 2024, with P7 and P9 at 0 mg N-NO_2^-/L and assigned to Class I, while the remaining sites were classified as Class II. All NO_3^- values also remained within Class I. However, NH_4^+ concentrations remained elevated, ranging from 11.23 ± 0.77 to 15.05 ± 0.09 mg N–NH_4^+/L, again resulting in Class V at every sampling point. Fe^{3+} remained at very low concentrations (0.0001-0.0004 mg Fe^{3+}/L), corresponding consistently to Class I.

A marked interannual difference was also observed for water TH. TH decreased from 190.66–251.23 mg/L in 2024 to 88.37–115.70 mg/L in 2025, with an especially pronounced reduction in CH, from 74.18-138.11 mg/L to approximately 10.72-12.10 mg/L.

Table 4. Physicochemical water-quality parameters for Herastrau Lake in 2025

Point	Temperature (°C)	pH (pH units)	EC (µS/cm)	Salinity (mg/L)	TDS (mg/L)	DO (mg O_2/L)	Turb. (NTU)	Cl^- (mg/L)
P1	13.01	8.59	657	320	332	3.30	4.36 ± 0.39	60.60 ± 3.48
P2	17.90	8.60	627	300	310	2.80	5.34 ± 0.45	57.29 ± 3.75
P3	13.07	8.58	683	340	347	3.70	9.88 ± 0.49	56.87 ± 1.17
P4	19.62	8.15	585	290	295	2.70	11.23 ± 1.12	54.31 ± 0.51
P5	13.06	8.95	670	330	335	2.60	11.60 ± 0.40	57.17 ± 0.46
P6	12.92	8.60	723	350	355	2.40	9.21 ± 0.28	56.54 ± 1.81
P7	11.90	8.84	607	300	303	2.20	7.06 ± 0.30	54.17 ± 0.89
P8	13.93	8.56	350	290	170	2.20	16.40 ± 0.71	52.56 ± 0.11
P9	12.54	8.50	601	290	301	2.10	7.41 ± 0.61	52.30 ± 0.20
P10	11.96	8.66	663	320	333	1.90	11.73 ± 0.47	57.24 ± 0.11
Point	**$N–NO_2^-$ (mg/L)**	**$N–NO_3^-$ (mg/L)**	**$N–NH_4^+$ (mg/L)**	**TSS (mg/L)**	**TH (mg/L)**	**CH (mg/L)**	**NCH (mg/L)**	**Fe^{3+} (mg/L)**
P1	0.05 ± 0.00	0.07 ± 0.00	11.23 ± 0.77	5.05 ± 0.22	115.70 ± 3.33	10.84 ± 0.20	104.86 ± 3.13	0.0004 ± 0.00
P2	0.05 ± 0.00	0.07 ± 0.00	14.68 ± 0.33	6.90 ± 0.16	101.92 ± 0.95	11.65 ± 0.08	90.27 ± 0.87	0.0003 ± 0.00
P3	0.04 ± 0.00	0.05 ± 0.00	12.22 ± 3.05	5.20 ± 0.08	98.45 ± 1.74	10.95 ± 0.20	87.50 ± 1.54	0.0003 ± 0.00
P4	0.04 ± 0.00	0.05 ± 0.00	13.21 ± 0.20	5.35 ± 0.07	101.36 ± 1.74	11.82 ± 0.16	89.54 ± 1.58	0.0003 ± 0.00
P5	0.04 ± 0.00	0.05 ± 0.00	13.94 ± 1.56	5.35 ± 0.16	103.82 ± 1.43	12.10 ± 0.08	91.73 ± 1.35	0.0003 ± 0.00
P6	0.03 ± 0.00	0.05 ± 0.00	12.95 ± 2.42	6.50 ± 0.08	99.57 ± 1.11	11.65 ± 0.08	87.92 ± 1.03	0.0003 ± 0.00
P7	0.00 ± 0.00	0.00 ± 0.00	14.70 ± 2.65	1.80 ± 0.06	95.98 ± 4.28	10.89 ± 0.12	85.09 ± 4.16	0.0002 ± 0.00
P8	0.03 ± 0.00	0.05 ± 0.00	15.05 ± 0.09	4.25 ± 0.53	88.37 ± 1.11	11.42 ± 0.32	76.94 ± 0.79	0.0001 ± 0.00
P9	0.00 ± 0.00	0.00 ± 0.00	12.36 ± 2.92	3.15 ± 0.43	95.87 ± 1.58	10.72 ± 0.04	85.15 ± 1.54	0.0003 ± 0.00
P10	0.04 ± 0.00	0.05 ± 0.00	14.69 ± 0.56	1.10 ± 0.28	99.90 ± 0.63	11.40 ± 0.20	88.51 ± 0.83	0.0003 ± 0.00

Table 5. Water-quality class assignment for Herastrau Lake in 2024 and 2025 campaigns

Point	DO	Cl^-	$N\text{-}NO_2^-$	$N\text{-}NO_3^-$	$N\text{-}NH_4^+$	Fe^{3+}
2024 monitoring campaign						
P1	Class I	Class I	Class III	Class I	Class V	Class I
P2	Class II	Class I	Class II	Class I	Class V	Class I
P3	Class II	Class I	Class II	Class I	Class V	Class I
P4	Class I	Class I	Class II	Class I	Class V	Class I
P5	Class I	Class I	Class II	Class I	Class V	Class I
P6	Class III	Class I	Class II	Class I	Class V	Class I
P7	Class II	Class I	Class II	Class I	Class V	Class I
P8	Class I	Class I	Class II	Class I	Class V	Class I
P9	Class I	Class I	Class II	Class I	Class V	Class I
P10	Class III	Class I	Class III	Class I	Class V	Class I
2025 monitoring campaign						
P1	Class V	Class I	Class II	Class I	Class V	Class I
P2	Class V	Class I	Class II	Class I	Class V	Class I
P3	Class V	Class I	Class II	Class I	Class V	Class I
P4	Class V	Class I	Class II	Class I	Class V	Class I
P5	Class V	Class I	Class II	Class I	Class V	Class I
P6	Class V	Class I	Class II	Class I	Class V	Class I
P7	Class V	Class I	Class I	Class I	Class V	Class I
P8	Class V	Class I	Class II	Class I	Class V	Class I
P9	Class V	Class I	Class I	Class I	Class V	Class I
P10	Class V	Class I	Class II	Class I	Class V	Class I

At the same time, the increase in EC and salinity in 2025 suggests that the seasonal change did not simply reflect a general dilution or concentration effect, but rather a modification in the ionic composition of the lake water.

Overall, the comparison between the two monitoring campaigns indicates that NH_4^+ was the most persistent water-quality issue, remaining in Class V throughout the lake in both years, while the most pronounced temporal deterioration concerned DO, which shifted from

Classes I-III in 2024 to Class V at all sites in 2025. Conversely, Cl^-, NO_3^-, and Fe^{3+} concentrations consistently remained within Class I. The simultaneous occurrence of high NH_4^+ concentrations and severe oxygen depletion in 2025 may indicate increased oxygen demand associated with organic matter and N transformations, suggesting enhanced eutrophication pressure within the lake.

Dippong and Resz (2024), in a study of lakes in the Tisa protected area in Romania, also reported generally adequate pH conditions, while EC varied widely from 213 to 1052 µS/cm. In Herastrau Lake, EC ranged from 331 to 547 µS/cm in 2024 and increased to 350-723 µS/cm in 2025, indicating a higher dissolved ionic load during the early-spring campaign. Another recent study of the Iza-Tisa (Romania) surface-water system reported EC values of 307-512 µS/cm, showing that the 2024 Herastrau Lake values were broadly comparable, whereas some 2025 sampling sites exhibited greater mineralization (Dippong & Resz, 2025).

The increase in EC in 2025 was linked to higher salinity, but hardness changed differently. TH dropped from 190.66-251.23 mg/L in 2024 to 88.37-115.70 mg/L in 2025, and CH fell sharply from 74.18-138.11 to 10.72-12.10 mg/L. Thus, the higher EC and salinity in 2025 do not originate solely from increased Ca- and Mg-hardness. Instead, these changes suggest a shift in the lake water's ionic composition between the two campaigns. Similar complexity in the relationships among EC, TDS, TH, and dissolved ions has been observed in other lake systems, where natural hydrogeochemical processes and anthropogenic inputs jointly determine water chemistry (Osman et al., 2025).

DO showed the most pronounced temporal variation. In autumn 2024, DO concentrations were Class I-III, but dropped dramatically in March 2025 to Class V. This decrease is notable because the 2025 campaign had lower water temperatures, suggesting oxygen deterioration is not driven by temperature effects alone. Recent research shows DO dynamics in shallow eutrophic lakes depend on interactions among water temperature, hydrological conditions, mixing, precipitation, wind, nutrients, and biological activity (F. Zhang et al., 2025). The generally well-oxygenated conditions in Romanian Tisa lakes highlight the poor oxygen conditions in Herastrau Lake in 2025 (Dippong & Resz, 2024).

Turbidity in northern Romanian lakes ranges from 0.68-48 NTU, highest in spring (Dippong & Resz, 2024). Values are lower than in highly turbid systems like Tonle Sap Lake, with an annual mean of 53.99 NTU and spring-summer means of 84.16 and 93.47 NTU. The autumn mean of 15.33 NTU is similar to Herastrau Lake. Turbidity responds to cropland, urbanization, and population density, reflecting anthropogenic impact (Zou et al., 2024).

Cl^- concentrations were comparatively stable in 2024 and 2025. Cl^- concentrations in Herastrau Lake are substantially lower than those reported for strongly salt-affected urban lakes. For example, Foley and Steinman (2023) reported Cl^- concentrations exceeding 230 mg/L and reaching about 331 mg/L in an urban lake affected by road deicing salts; these concentrations were high enough to interfere with lake mixing and contribute to hypolimnetic hypoxia.

In contrast, ammonium represented the most critical nitrogen-related parameter. The NH_4^+ values of Herastrau Lake are markedly higher than those reported for other Romanian lake systems. Dippong et al. (2024) reported a maximum NH_4^+ concentration of approximately 1.79 mg/L in polluted lakes from northern Romania. The elevated ammonium levels observed in Herastrau Lake may reflect the strong anthropogenic pressure characteristic of its urban catchment.

The concurrent occurrence of persistently high ammonium concentrations and pronounced dissolved oxygen depletion in 2025 may indicate increased eutrophication and organic/nitrogen loading pressure. Global lake datasets identify NH_4^+, NO_3^-/NO_2^-, DO, turbidity, TSS, and EC as key indicators for characterizing lake ecological condition, with elevated NH_4^+ often associated with anthropogenic pollution and adverse effects on aquatic organisms (Naderian et al., 2024).

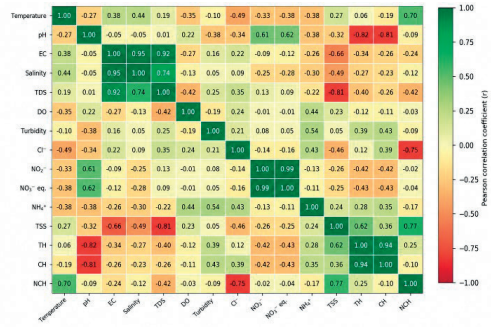
Overall, the results suggest two different physicochemical conditions between the monitoring campaigns. The 2024 campaign was characterized by moderately mineralized, slightly alkaline and relatively well-oxygenated water, despite consistently high NH_4^+ concentrations. In 2025, the lake exhibited

increased EC and salinity, substantially reduced CH and TH, persistently elevated NH_4^+ and, most importantly, severe oxygen depletion throughout the sampling network. These multidimensional changes are characteristic of urban lake systems, where hydrological conditions, seasonal processes, and anthropogenic inputs interact to control water quality.

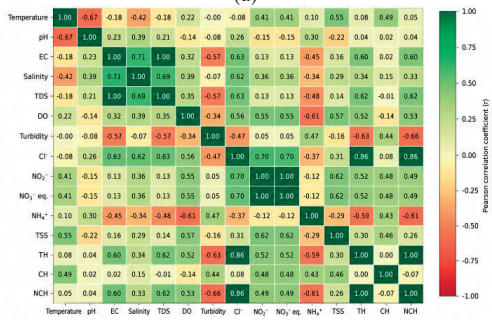
Pearson Correlation Analysis

In 2024, the Pearson correlation analysis identified several clear relationships among the physicochemical parameters (Figure 2a). EC was strongly positively correlated with salinity (r = 0.95) and TDS (r = 0.92), while salinity was also positively related to TDS (r = 0.74), indicating these parameters reflect a common variation in the lake's dissolved ionic content. TH and CH showed a strong positive correlation (r = 0.94). Conversely, pH was strongly negatively correlated with TH (r = -0.82) and CH (r = -0.81). TSS showed a strong negative correlation with TDS (r = -0.81) and a moderate negative correlation with EC (r = -0.66), while it was positively correlated with NCH (r = 0.77). Cl^- displayed a marked negative correlation with NCH (r = -0.75). NH_4^+ showed moderate positive relationships with turbidity (r = 0.54), DO (r = 0.44), and Cl^- (r = 0.43), indicating its spatial distribution is linked to multiple physicochemical characteristics rather than a single factor. The correlation pattern changed markedly in 2025 (Figure 2b). EC and TDS were nearly perfectly correlated (r ≈ 1.00), and both remained positively associated with salinity, confirming their close dependence on dissolved mineral content. Cl^- showed strong positive correlations with both TH and NCH (r = 0.86) and was also positively related to NO_2^- and NO_3^- concentrations (r = 0.70).

In contrast, turbidity was negatively correlated with NCH (r = -0.66), TH (r = -0.63), EC (r = -0.57), and TDS (r = -0.57), indicating that areas with greater optical effects from suspended particles did not necessarily coincide with those with the highest dissolved ionic content. A particularly relevant relationship was observed between DO and NH_4^+ (r = -0.61). Higher NH_4^+ concentrations were therefore associated with lower DO values across the sampling sites, consistent with increased oxygen demand from organic-matter degradation and nitrogen transformation processes. NH_4^+ was also negatively correlated with TH (r = -0.59) and NCH (r = -0.61).



(a)



(b)

Figure 2. Pearson correlation matrix of physicochemical water-quality parameters in Herastrau Lake in (a) 2024 and (b) 2025 monitoring campaigns

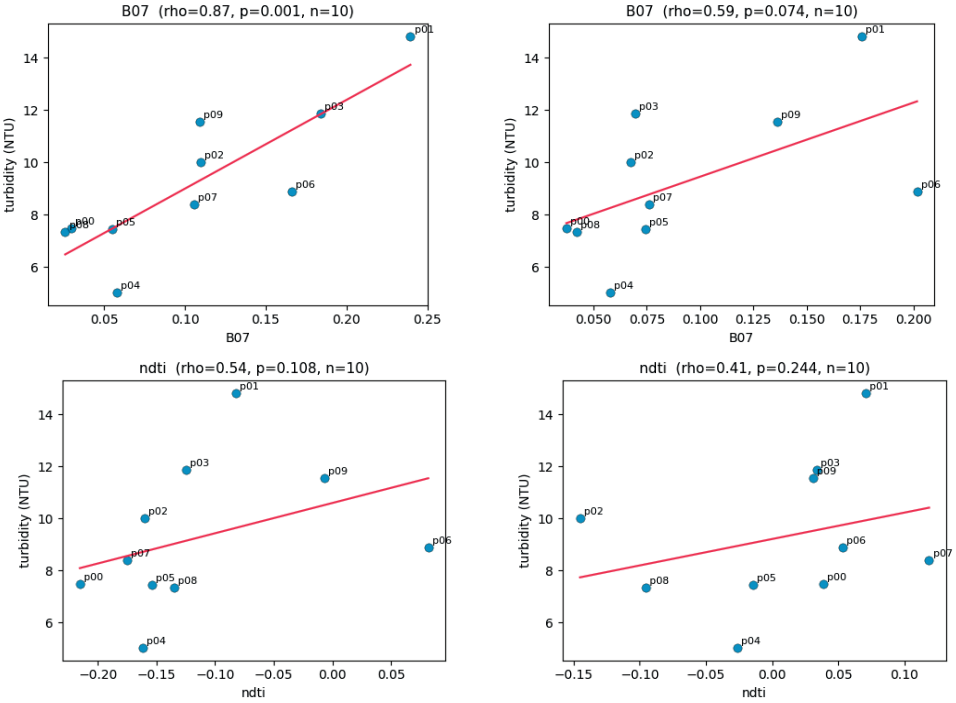
The different correlation structures observed in the two campaigns reveal a clear temporal shift in the relationships among the measured water-quality variables. In 2024, the strongest correlations were mainly linked to mineralization, hardness, and suspended solids. By 2025, the correlations involving DO, NH_4^+, Cl^-, and turbidity became more prominent. These variations suggest seasonal changes in the processes governing water chemistry, potentially reflecting differences in hydrological conditions, external inputs, biological activity, and nutrient cycling within Herastrau Lake.

Satellite-Based Turbidity Assessment and Calibration

Conventional in-situ monitoring, although accurate, is labor-intensive, costly, and inherently limited in spatial and temporal coverage, typically yielding few point samples

collected infrequently. Satellite remote sensing offers a complementary approach: Sentinel-2 provides spatially continuous, frequently revisited (≈5-day) and openly available imagery that can capture the entire water surface synoptically. However, satellite-derived water-quality estimates are reliable only after calibration and validation against ground-truth measurements. In this study, the optically active parameter turbidity was estimated from Sentinel-2 reflectance and validated against in-situ data; once validated in this way, the calibrated satellite proxies can be applied operationally to map turbidity (and, by extension, chlorophyll a) across the whole lake and to track its dynamics over time, at low cost and with a spatial and temporal resolution that point sampling alone cannot achieve. This integration of field measurements with validated remote sensing is the core methodological rationale of the present work.

As shown in Figure 3, although NDTI is specifically designed as a turbidity index, it did not perform as expected: it showed only weak, non-significant correlations with in-situ turbidity in both campaigns.



a) October 2024 campaign ***b) March 2025 campaign***

Figure 3. Spatial relationship between in-situ turbidity and two Sentinel-2 turbidity predictors, band B07 (783 nm, top row) and the Normalized Difference Turbidity Index (NDTI, bottom row), across the ten sampling points, for (a) the October 2024 campaign and (b) the March 2025 campaign. The red line shows the linear fit; Spearman correlation coefficients (ρ) and p-values are reported in each panel. B07 was the strongest predictor in both campaigns, with a significant correlation in October (ρ = 0.87, *p* = 0.001) but a weaker, non-significant one in March (ρ = 0.59, *p* = 0.074); NDTI performed poorly in both periods

This underperformance likely reflects the strong influence of algal/chlorophyll signals in the eutrophic lake, which interfere with the red–green contrast on which NDTI relies.

The contrast between the two predictors is itself informative about the optical regime of the lake. NDTI relies on the red-versus-green contrast and was developed for small, mineral-dominated ponds (Lacaux et al., 2007), where that contrast tracks inorganic suspended sediment. In a chlorophyll-rich system the same contrast is confounded, since phytoplankton absorbs strongly in the red (~665 nm) while pigment absorption and cell scattering also

modify the green signal, so both bands respond to algal biomass rather than to sediment load. That the turbidity information was carried instead by the red-edge region, beyond the main pigment absorption features, is consistent with the hypereutrophic character indicated by the physicochemical data, and points to red-edge-based indices such as NDCI (Mishra & Mishra, 2012) as the appropriate route for extending this approach to chlorophyll-a retrieval in Herastrau Lake.

Once band B07 had been selected as the turbidity predictor, three calibration models were fitted to relate B07 surface reflectance to the in-situ turbidity measurements: (i) a linear model (T = a·B07 + b), the simplest empirical formulation; (ii) a power model (T = a·B07^b), which can better accommodate the non-linear, saturating behavior often observed in turbidity–reflectance relationships; and (iii) the semi-analytical Nechad model (T = A·ρ/(1 - ρ/C)) (Nechad et al., 2010), a physically based formulation widely used for turbidity retrieval from water-leaving reflectance. The performance of each model was assessed using the coefficient of determination (R^2) and the root-mean-square error (RMSE), as shown in Figures 4 and 5.

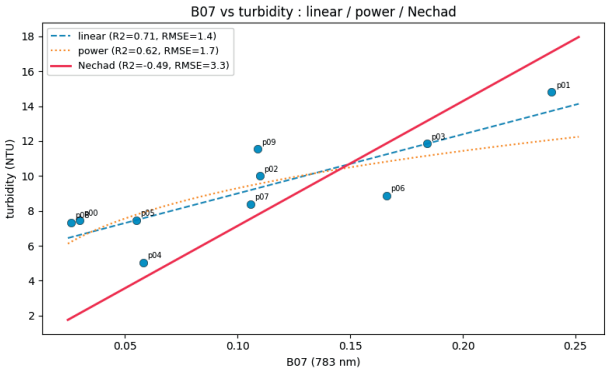


Figure 4. Calibration of the Sentinel-2 turbidity proxy for the October 2024 campaign: in-situ turbidity (NTU) at the ten sampling points versus Sentinel-2 band B07 (783 nm) surface reflectance. Three regression models are shown: linear (R^2 = 0.71, RMSE = 1.4 NTU), power (R^2 = 0.62, RMSE = 1.7 NTU), and the semi-analytical Nechad model (R^2 = −0.49, RMSE = 3.3 NTU). The linear model provided the best fit and was retained; the Nechad model failed to reproduce the lake's high background turbidity

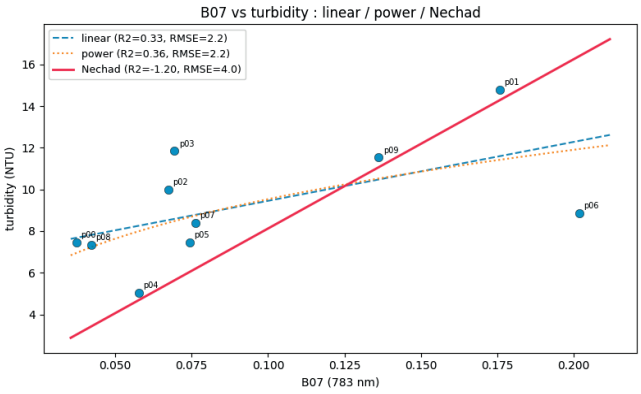


Figure 5. Calibration of the Sentinel-2 turbidity proxy for the March 2025 (early-spring) campaign: in-situ turbidity (NTU) at the ten sampling points versus Sentinel-2 band B07 (783 nm) surface reflectance, with linear (R^2 = 0.33, RMSE = 2.2 NTU), power (R^2 = 0.36, RMSE = 2.2 NTU) and semi-analytical Nechad (R^2 = −1.20, RMSE = 4.0 NTU) regression fits. In contrast to the October campaign (R^2 = 0.71), the B07–turbidity relationship was markedly weaker and statistically non-significant (Spearman ρ = 0.59, p = 0.074), most likely owing to the larger time lag between the satellite acquisitions and the sampling date

In contrast to the autumn campaign, the B07–turbidity relationship for March 2025 was considerably weaker and non-significant (Figure 5). The most likely cause is the match-up window: in October, a cloud-free scene coincided with the sampling day, whereas the March composite was built from scenes acquired 6 and 9 days from sampling, over which surface turbidity in this shallow, wind-exposed lake can change appreciably through resuspension and settling. A shift in particle composition may also contribute, as the early-spring increase in the algal fraction alters the reflectance-to-NTU relationship. The March retrieval is therefore regarded as exploratory.

CONCLUSIONS

The water-quality parameters measured in this study, including elevated ammonium concentrations, markedly reduced dissolved oxygen, and persistent turbidity above 5 NTU, are consistent with sustained eutrophication pressure. Regular monitoring is thus essential to detect degradation early, understand its spatial and temporal dynamics, and inform targeted management and pollution-control measures.

A key limitation of this study stems from the use of Sentinel-2 Level-2A (Sen2Cor) reflectance, whose atmospheric correction is optimized for land surfaces rather than water. Over water bodies, this often results in weak or even negative reflectances and leaves residual sun-glint uncorrected, limiting the absolute accuracy of the retrieved values. The turbidity estimates derived here should therefore be regarded as semi-quantitative, and negative reflectances over water should be screened and treated with caution. For more rigorous, quantitative turbidity retrieval, dedicated aquatic atmospheric-correction processors such as ACOLITE, C2RCC, or POLYMER would be required, and their application represents a promising direction for future work.

ACKNOWLEDGEMENTS

This work was supported by a grant of the Ministry of Education and Research, CCCDI-UEFISCDI, project number PN-IV-P6-6.1-CoEx-2024-0120, within PNCDI IV.

Mihaela Dragoi Cudalbeanu and Daniela Faur express their gratitude to the Romanian-American Foundation and the Romanian Fulbright Commission for the opportunity to participate in the Fulbright-RAF Scholar Award.

REFERENCES

Cheval, S., Popa, A. M., Şandric, I., & Iojă, I. C. (2020). Exploratory analysis of cooling effect of urban lakes on land surface temperature in Bucharest (Romania) using Landsat imagery. Urban Climate, 34, 100696. https://doi.org/10.1016/J.UCLIM.2020.100696.

Dippong, T., & Resz, M.-A. (2024). Heavy metal contamination assessment and potential human health risk of water quality of lakes situated in the protected area of Tisa, Romania. Heliyon, 10(7), e28860. doi:10.1016/j.heliyon.2024.e28860.

Dippong, T., & Resz, M.-A. (2025). Water and sediments pollution from Iza River (Romania): Influence on water quality and metals content. Process Safety and Environmental Protection, 200, 107335. doi:10.1016/j.psep.2025.107335.

Dippong, T., Senila, M., Cadar, O., & Resz, M.-A. (2024). Assessment of the heavy metal pollution degree and potential health risk implications in lakes and fish from northern Romania. Journal of Environmental Chemical Engineering, 12(2), 112217. doi:10.1016/j.jece.2024.112217.

Foley, E., & Steinman, A. D. (2023). Urban lake water quality responses to elevated road salt concentrations. Science of the Total Environment, 905, 167139. doi:10.1016/j.scitotenv.2023.167139.

Hoggang, G.C.B., & Reyes, A. T. (2023). Physico-chemical and biological water quality analysis of Ambuwaya Lake in Kiangan, Ifugao, Philippines. *AACL Bioflux*, 16(6).

Lacaux, J. P., Tourre, Y. M., Vignolles, C., Ndione, J. A., & Lafaye, M. (2007). Classification of ponds from high-spatial resolution remote sensing: Application to Rift Valley Fever epidemics in Senegal. Remote Sensing of Environment, 106(1), 66–74. https://doi.org/10.1016/j.rse.2006.07.012.

Liu, D., Zhang, C., Yan, N., Yan, Y., & Duan, H. (2025). Eutrophication exacerbated organic pollution in lakes across China during the 1980s–2010s. Water Research, 268. https://doi.org/10.1016/j.watres.2024.122782.

McFeeters, S. K. (1996). The use of the Normalized Difference Water Index (NDWI) in the delineation of open water features. International Journal of Remote Sensing, 17(7), 1425–1432. https://doi.org/10.1080/01431169608948714

Mishra, S., & Mishra, D. R. (2012). Normalized difference chlorophyll index: A novel model for remote estimation of chlorophyll-a concentration in turbid productive waters. Remote Sensing of Environment, 117, 394-406. https://doi.org/10.1016/j.rse.2011.10.016.

Morelato, R. R., Rodrigues-Silva, F., Viana, G. C. C., & Amorim, C. C. (2026). Advancing eutrophication mitigation through nature-based and hybrid solutions: A systematic review. Journal of Environmental Chemical Engineering, 14(1), 121046. https://doi.org/10.1016/j.jece.2026.121046.

Naderian, D., Noori, R., Heggy, E., Bateni, S. M., Bhattarai, R., Nohegar, A., & Sharma, S. (2024). A water quality database for global lakes. Resources, Conservation and Recycling, 202, 107401. doi:10.1016/j.resconrec.2023.107401.

Nechad, B., Ruddick, K. G., & Park, Y. (2010). Calibration and validation of a generic multisensor algorithm for mapping of total suspended matter in turbid waters. Remote Sensing of Environment, 114(4), 854–866. https://doi.org/10.1016/j.rse.2009.11.022.

Nkhata, A. D., Mengistou, S., & Gondwe, L. S. M. (2026). Linking water quality with plankton dynamics: multivariate analyses of environmental drivers in Lake Koka. Journal of Freshwater Ecology, 41(1). https://doi.org/10.1080/02705060.2026.2626169.

Osman, K. A., Elgendy, S. M., & Ibrahim, H. Z. (2025). Physicochemical and spatial distributions of trace elements and organochlorine compounds in Lake Idku water, Egypt. Water, Air, & Soil Pollution, 236, 127. https://doi.org/10.1007/s11270-025-07757-x.

Oustani, M., Mehda, S., Rekbi, F. M. L., Guezie, R., Youcef, F., Halilat, M. T., Debba, S., & Chenchouni, H. (2026). Physicochemical, biochemical and bacteriological indicators of water quality of Temacine Lake in the Sahara Desert. Environmental Nanotechnology, Monitoring and Management, 25. https://doi.org/10.1016/j.enmm.2026.101143.

Sandu, M. A., Vîrsta, A., Vasile Scăeţeanu, G., Iliescu, A.-I., Ivan, I., Nicolae, C. G., Stoian, M., & Madjar, R. M. (2023). Water quality monitoring of Moara Domnească Pond, Ilfov County, using UAV-based RGB imaging. AgroLife Scientific Journal, 12(1), 191–201.

Zhang, F., Shi, X., Zhao, S., Arvola, L., Sun, B., Hao, R., Yang, Z., Wang, S., Zhao, Y., & Zhang, J. (2025). Dissolved oxygen dynamics in a shallow eutrophic lake: Quantify critical eco-environmental effects. Ecological Indicators, 179, 114190. doi:10.1016/j.ecolind.2025.114190.

Zhang, K., Li, M., Qu, S., Zhao, Y., Duan, L., Yang, X., Li, D., Liao, Z., & Yu, R. (2025). Spatio-seasonal variability of source contributions to water quality in a large irrigation drainage lake basin based on the entropy weighted quality index, positive matrix factorization, and isotopic tracers. Environmental Pollution, 382, 126670. https://doi.org/10.1016/J.ENVPOL.2025.126670.

Zhou, J., Mogollón, J. M., Van Bodegom, P. M., Beusen, A. H., & Scherer, L. (2024). Global regionalized characterization factors for phosphorus and nitrogen impacts on freshwater fish biodiversity. Science of The Total Environment, 912, 169108. https://doi.org/10.1016/j.scitotenv.2023.169108.

Zou, T., Yang, K., Pan, M., Zhu, Y., Zhang, Y., & Su, D. (2024). Analysis of the temporal and spatial evolution of turbidity in Tonle Sap Lake and its influencing factors. Science of the Total Environment, 943, 173618. doi:10.1016/j.scitotenv.2024.173618.

*International Organization for Standardization (2016). ISO 5667-4:2016 Water quality - Sampling - Part 4: Guidance on sampling from lakes, natural and man-made. International Organization for Standardization.

**Ministry of Environment and Water Management (2006). Order No. 161/2006 approving the normative regarding the classification of surface water quality for establishing the ecological status of water bodies. Official Gazette of Romania, No. 511/13 June 2006.